ELSEVIER

The structure of *p*-chlorophenol and barrier to internal ─OH rotation in the S_1-state

Marcel Böhm, Christian Ratzer, Michael Schmitt *

Heinrich-Heine-Universität, Institut für Physikalische Chemie, D-40225 Düsseldorf, Germany

Abstract

The structure and barrier to internal rotation of 4-chlorophenol in the ground state and the electronically excited S_1-state has been examined by rotationally resolved laser induced fluorescence spectroscopy of 4-^{35}Cl-phenol, 4-^{37}Cl-phenol, 4-^{35}Cl-phenol-d_1, and 4-^{37}Cl-phenol-d_1. The overlapping spectra have been assigned simultaneously using a genetic algorithm approach. The rotationally resolved spectrum of the electronic origin of 4-chlorophenol is comprised of two subbands, which are split by 60 MHz due to the internal rotation of the hydroxy group. The torsional barrier in the electronically excited state could be estimated to be 1400 cm^{-1}, only about 250 cm^{-1} higher than in the ground state. The C─Cl bond lengths decreases by approximately 6 pm upon electronic excitation and the aromatic ring is distorted quinoidally.
© 2006 Elsevier B.V. All rights reserved.

1. Introduction

As has been pointed out by Zierkiewicz et al., the knowledge of torsional barriers in the electronic ground state "reveals important information about the nature of bonding and the extent of conjugation in aromatic systems" [1]. This statement is especially true for electronically excited states, in which the electronic structures are largely altered compared to the ground state. In two preceding studies we investigated the excited state torsional barrier of the hydroxy group in *p*-fluorophenol [2] and *p*-cyanophenol [3]. Substituents in *para* position to the hydroxy group have the advantage of being electronically coupled to the hydroxy group, but do not exert a sterical effect on the torsional barrier. In the present publication we extend our investigations to *p*-chlorophenol. Compared to fluorophenol, in which only an inductive effect of the substituent is observed, chlorine also exerts a mesomeric effect. The tor-

sional barrier of *p*-chlorophenol is estimated in the electronically excited state and the structural changes upon electronic excitation are determined.

The torsional barrier of 4-chlorophenol (4-fluorophenol) in the electronic ground state has been determined by Larsen to be 1148 (1006) cm^{-1} using microwave spectroscopy [4]. Fateley et al. [5] measured the torsional frequencies of various para-substituted phenols in the far-infrared and could show that the torsional frequencies are directly related to the electron-donating or -withdrawing power of the substituent group. Cvitaš et al. examined structural changes of several mono- and disubstituted benzenes upon electronic excitation from their rotational band contours in the electronic spectra [6–10]. Christoffersen et al. [11] fitted the rotational constants of *p*-fluoroaniline and *p*-fluorophenol to the band contour in the electronic spectrum and reported the rotational constants of ground and excited electronic states.

A Franck–Condon analysis of the emission spectra of 4-chlorophenol has been performed by Imhof et al. [12]. They found an overall increase in the C─C bond lengths of the aromatic ring, and a decrease of the C─Cl and the

---

C—O bond lengths upon electronic excitation. These results were compared to structural changes calculated at CASSCF level.

The torsional barriers of various *p*-halogenophenols in the electronic ground state have been investigated theoretically by Zierkiewicz et al. [1]. Based on a natural bond orbital analysis they postulated that the barrier height in *p*-halogenophenols is caused by the decrease of electron density in the sigma antibonding orbital, σ^* of the C—O bond.

2. Experimental setup

The experimental setup for the rotationally resolved laser induced fluorescence is described in detail elsewhere [13]. Briefly, it consists of a ring dye laser (Coherent 899-21) operated with Rhodamine 110, pumped with 6 W of the 514 nm line of an Ar^+-ion laser. The light is coupled into an external folded ring cavity (Spectra Physics) for second harmonic generation. The molecular beam is formed by expanding *p*-chlorophenol heated to 140 °C and seeded in 700 mbar of argon through a 100 μm hole into the vacuum. The molecular beam machine consists of three differentially pumped vacuum chambers that are linearly connected by two skimmers (1 and 3 mm, respectively) in order to reduce the Doppler width. The molecular beam is crossed at right angles in the third chamber with the laser beam 500 mm downstream of the nozzle. The resulting fluorescence is collected perpendicular to the plane defined by laser and molecular beam by an imaging optics setup consisting of a concave mirror and two plano-convex lenses. The resulting Doppler width in this setup is 15 MHz (FWHM). The integrated molecular fluorescence is detected by a photo-multiplier tube whose output is discriminated and digitized by a photon counter and transmitted to a PC for data recording and processing. The relative frequency is determined with a quasi confocal Fabry–Perot interferometer. The absolute frequency was determined by recording the iodine absorption spectrum and comparing the transitions to the tabulated lines [14]. 4-Chlorophenol was purchased from Fluka and was used without further purification. 4-Chlorophenol-d_1 was prepared from 4-chlorophenol by refluxing with an excess of D_2O for three times and subsequent removal of the solvent. This procedure resulted in an isotopic purity of >95%.

3. Theoretical methods

The structure of *p*-chlorophenol in the electronic ground state has been optimized at the HF/6-31G(d,p), B3LYP/6-31G(d,p), and MP2/6-31G(d,p) levels for the electronic ground state and at the CIS/6-31G(d,p) and CASSCF/6-31G(d,p) levels for the electronically excited S_1-state with the Gaussian 98 program package (Revision11) [15]. The SCF convergence criterion used throughout the calculations was an energy change below 10^{-8} Hartree, while the convergence criterion for the gradient optimization of

the molecular geometry was $\partial E/\partial r < 1.5 \times 10^{-5}$ Hartree/Bohr and $\partial E/\partial \varphi < 1.5 \times 10^{-5}$ Hartree/degrees, respectively. The CASSCF optimization has been performed with ten electrons in ten orbitals. The active space is comprised of the three aromatic π, π^* orbitals located at the benzene ring, one p_z orbital at the phenolic oxygen atom, and one p_z orbital at the chlorine atom.

4. The genetic algorithms

We used an automated fitting procedure for the rovibronic spectra, based on a genetic algorithm fit, which is described in detail in Refs. [16,17]. The GA library PGA-Pack version 1.0 is used, which can run on parallel processors [18]. For the simulation of the rovibronic spectra a rigid asymmetric rotor Hamiltonian was employed [19]. The genetic algorithm copies concepts from evolutionary processes like sexual reproduction, selection, and mutation. For a detailed description of the GA as fitting algorithms the reader is referred to the original literature on evolutionary or genetic algorithms [20–22].

5. Results and discussion

Fig. 2 shows part of the rotationally resolved LIF spectrum of the electronic origin $\widetilde{A}^1B_2 \leftarrow \widetilde{X}^1A_1$ of 4-chlorophenol at 34809.8 cm^{-1}. The spectrum is comprised of two band systems due to the isotopomeric ^{35}Cl-phenol and ^{37}Cl-phenol species in their natural abundance of 3:1. Furthermore the spectrum consists of two subbands, which are separated by approximately 60 MHz. This splitting can be traced back to the hindered internal motion of the hydroxy group about the C_1O_7 bond, which will be discussed in detail in Section 5.1. The atomic numbering used in this publication is shown in the left part of Fig. 1 .

The four subspectra have been fit simultaneously, using the GA procedure, which is described in detail in Refs. [16,17]. 4-Chlorophenol is a near prolate asymmetric rotor in both electronic states as can be seen from its κ-value of −0.9400 for ^{35}Cl-phenol and of −0.9431 for ^{37}Cl-phenol in the S_0-state and of −0.9300(−0.9345) in the S_1-state, cf. Table 1. The rotational temperature, taking nuclear spin
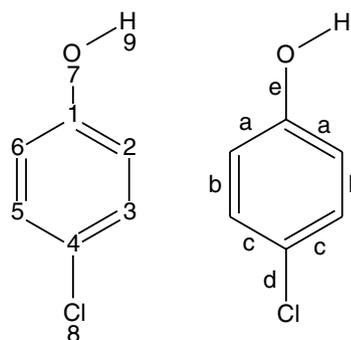

Fig. 1. Atomic numbering of *p*-chlorophenol and model used in the structural fits.
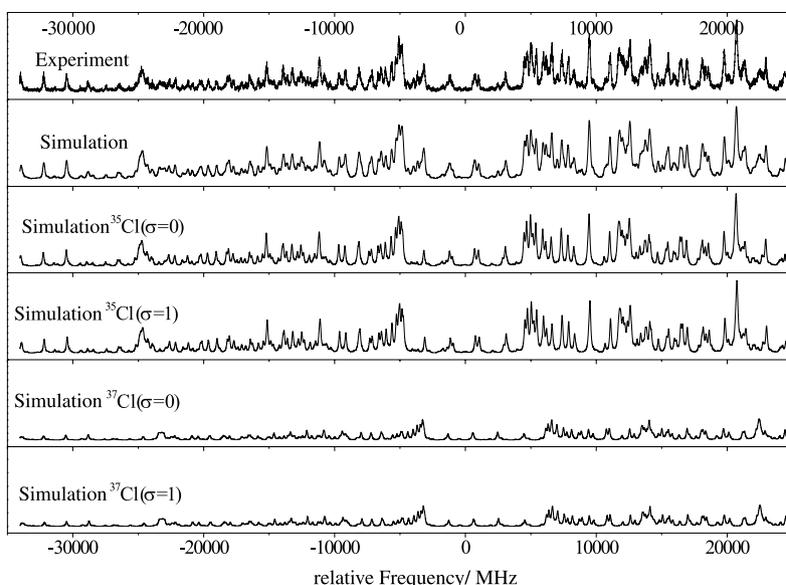
Fig. 2. Rotationally resolved spectra of the electronic origin of 4-^{35}chlorophenol and 4-^{37}chlorophenol together with the simulation of the two torsional subbands of each isotopomer using the molecular constants given in Table 1. The subbands are labeled with 0^+ for the $\sigma = 0$ component of the vibronic ground state and with 0^- for the $\sigma = 1$ component.

Table 1
Molecular constants of 4-^{35}chlorophenol, 4-^{37}chlorophenol, 4-^{35}chloro-[7-D]phenol and 4-^{37}chloro-[7-D]phenol obtained from the GA fit to the experimental spectra

	^{35}Chlorophenol	^{37}Chlorophenol	^{35}Chlorophenol-d_1	^{37}Chlorophenol-d_1
A''/MHz	5632.777	5632.766	5591.009	5591.7(16)
B''/MHz	975.5696	950.4789	951.8543	928.01(41)
C''/MHz	831.6534	813.3499	813.5048	796.17(55)
ΔI/uÅ^2	−0.0761	−0.0762	−0.0963	−0.2007
κ	−0.9400	−0.9431	−0.9421	−0.9450
A'/MHz	5289.01(18)	5288.08(48)	5250.11(43)	5248.5(25)
B'/MHz	990.27(6)	963.73(37)	966.29(3)	942.35(11)
C'/MHz	834.40(2)	817.32(15)	816.54(4)	799.33(10)
ΔI/uÅ^2	−0.2207	−1.6271	−0.3452	−0.3323
κ	−0.9300	−0.9345	−0.9324	−0.9357
v/cm^{-1}	34809.81(2)	34809.86(2)	34804.02(2)	34804.07(2)
Δv_{sub}/MHz	60(5)	67(2)	–	–
$\Delta v_{Lorentz}$/MHz	147(4)	147(4)	98(3)	98(3)

The ground state rotational constants of the first three isotopomers have been taken from Ref. [4].

statistics into account, is determined to be 0.75 K. The G_4-symmetric 4-chlorophenol exhibits a 10:6 spin statistic for $K_a(even):K_a(odd)$ for transitions of the torsional ground state $\sigma = 0$, and 6:10 for the torsionally excited state $\sigma = 1$. The Lorentzian contribution to the total line width with a Gaussian contribution of 15 MHz is determined to be 147 ± 20 MHz, yielding an excited state life time of 1.0 ± 0.3 ns.

Fig. 3 shows the rotationally resolved LIF spectrum of the electronic origin of 4-^{35}chlorophenol-d_1 and 4-^{37}chlorophenol-d_1 at 34804.0 cm^{-1}. The origin band of the deuterated isotopomer is red-shifted by 5.8 cm^{-1}, a value larger than in phenol (1.8 cm^{-1}), and of similar size as in p-fluorophenol (7.4 cm^{-1}). Since the torsional splitting in the electronic ground state, determined by microwave spectroscopy, amounts only to 0.376 MHz [4], we were

not able to resolve the torsional splitting, with a Gaussian contribution to the linewidth of 15 MHz and a Lorentzian width of 98 ± 10 MHz. This linewidth accounts for an excited state life time of 1.6 ± 0.2 ns, slightly larger than for the undeuterated species.

5.1. Barrier to hydroxy group torsion

The torsional splitting ($0^+/0^-$) of 4-chlorophenol in the electronic ground state has been determined by microwave spectroscopy to be 79.5 MHz [4]. The line splitting observed in the LIF spectrum amounts to 60 ± 10 MHz, cf. Table 1. Together with the selection rule $\Delta\sigma = \pm 1$, the torsional level splitting in the electronically excited state can be determined to be 20.0 ± 10 MHz. The torsional transition $1 \leftarrow 0^\pm$ has been reported by Fateley et al. to
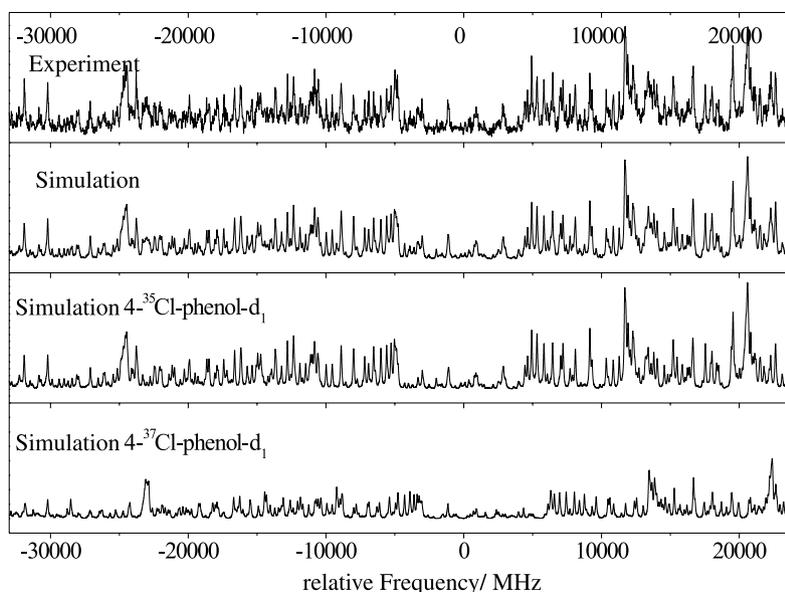
Fig. 3. Rotationally resolved spectra of the electronic origin of 4-^{35}chlorophenol-d_1 and 4-^{37}chlorophenol-d_1 together with the simulation using the molecular constants given in Table 1.

be 303 cm^{-1} [5]. Using these values and a torsional constant F of 690 GHz (as in the electronic ground state), the torsional S_1-barrier is calculated to be 1400 ± 200 cm^{-1}. In Table 2 the barriers to internal rotation of the hydroxy group in 4-chlorophenol, 4-fluorophenol, phenol, 4-cyanophenol, and 4-methylphenol are summarized for both electronic states.

5.2. Determination of the structure

The program *pKrFit* [23] was used to determine the intermolecular structure of the phenol dimer in the S_0 and S_1-state from the rotational constants, given in Table 1. *pKrFit* uses a gradient-based χ^2 minimizer as well as a GA-based global optimizer [24]. The GA library [18] was used in minimization mode and thus directly used the correspondingly defined χ^2 value as cost function. Due to the limited number of inertial parameters, several constraints to the geometry were necessary. Two different models have been used. Model I is depicted in the right part of Fig. 1. "Ortho" (a), "meta"(b), and "para"(c) bonds of the aromatic rings are set equal and are fit. Furthermore, the

C_4Cl_8 (d), the C_1O_7 (e) bond lengths, the $C_2C_1O_7$, and $C_1O_7H_{7a}$ angles are fit. In model II all CC ring bonds are treated as being equal and a mean aromatic CC bond length is fit. Furthermore, the C_4Cl_8 (d), the C_1O_7 (e) bond lengths are fit. Table 3 compares the results for the two models. For the electronic ground state a mean CC_{ar} bond length of 139.8 pm is found for both models. The C_4Cl_8 bond length is determined to be 172.8 pm in quite good agreement with the value given by Larsen of 172.04 pm. The C_1O_7 bond length differs slightly between the two models (136.5 pm using model I and 135.9 pm using model II).

The mean CC_{ar} bond length increases to 143.8 pm using model I and to 144.9 pm using model II upon electronic excitation. Model I shows a distinct quinoidal structure, with longer C_2C_3, C_1O_7, and C_4Cl_8 bonds and a shorter C_2C_3 bond. In both models the O_7H_{7a} and the C_4Cl_8 bonds are considerably shortened upon electronic excitation.

In addition, we determined the position of the hydroxylic H-atom and of the chlorine atom via a Kraitchman analysis. The moments of inertia of the planar 4-chlorophenol, which are used in the Kraitchman equations [25,26], are

Table 2
Barriers to internal rotation of 4-chlorophenol, 4-fluorophenol, phenol, 4-cyanophenol, and 4-methylphenol

State	4-Chlorophenol	4-Fluorophenol	Phenol	4-Cyanophenol	4-Methylphenol
S_0	1148[a]	1006[a]	1213[b]	1420[c]	1130[d]
S_1	1400[e]	1820[f]	4710[g]	⩾5000[c]	4395[d]

[a] From microwave spectra of Ref. [4].
[b] From microwave spectra of Ref. [27].
[c] From rotationally resolved electronic spectroscopy of Ref. [3].
[d] From rotationally resolved electronic spectroscopy of Ref. [28].
[e] This work.
[f] From rotationally resolved electronic spectroscopy of Ref. [2].
[g] From rotationally resolved electronic spectroscopy of Ref. [29].

Table 3

Experimental r_0-geometry parameters (distances in pm and angles in degrees) of 4-chlorophenol, obtained from a fit of the geometry to the experimental inertial parameters

	S_0		S_1	
	Model I	Model II	Model I	Model II
C_1C_2	140.0(9)	139.8(1)	146.5(9)	144.9(1)
C_2C_3	139.8(1)	139.8(1)	141.7(20)	144.9(1)
C_3C_4	139.5(9)	139.8(1)	143.3(9)	144.9(1)
C_4Cl_8	172.8(3)	172.8(2)	165.3(26)	164.4(10)
C_1O_7	136.5(2)	135.9(3)	130.0(30)	124.3(16)
O_7H_{7a}	96.0	96.0	98.0	98.0
$C_{ar}H$	108.1	108.1	107.2	107.2
CCC_{ar}	120	120	120	120
CCH	120	120	120	120
$C_3C_4Cl_8$	120	120	120	120
$C_2C_1O_7$	124(2)	122	122	122
$C_1O_7H_{7a}$	106(2)	110	110	110

calculated from the A and B rotational constants, given in Table 1. Table 4 summarizes the substitution coordinates for 4-chlorophenol, 4-fluorophenol, and phenol.

Using the *pseudo-*r_s structure of phenol from Ref. [23] for the ground state and replacing the H-atom in para position with a chlorine atom, we fitted the C_4Cl_8 distance, until the substitution coordinate of chlorine in *p*-chlorophenol was matched. In this way a C—Cl distance of 172.9 pm was obtained. This value differs from the bond length of 172.04, which was calculated by Larsen on the basis of the full Kraitchman substitution structure for the phenol moiety [4]. We took the less accurate values from the *pseudo-*r_s analysis from Ref. [23], since in a subsequent step the C—Cl bond length in the electronically excited state was determined, for which the *pseudo-*r_s structure of the excited state of phenol was needed. For the excited state a C—Cl distance of 166.9 pm was calculated, which is a reduction of 6.0 pm upon electronic excitation. Both ground and excited state C—Cl bond lengths agree well with the values obtained from the fit of the structure to the rotational constants.

5.3. Comparison to the results of ab initio calculations

Table 5 shows a comparison of the experimentally determined inertial and geometrical parameters of the ^{35}Cl isotopomer of chlorophenol with the corresponding ab initio values. For the ground state a very close agreement

between the MP2/6-31G(d,p) calculated rotational constants and the experimental ones is found. Also the experimental structural parameters, that are taken from model I in Section 5.2, are in good agreement with the calculated ones.

The change of rotational constants upon electronic excitation can be nicely predicted by taking the difference of the CIS and HF calculations using the same basis sets. Due to the deficiencies of both methods, mainly the lack of electron correlation, the absolute values of the rotational constants differ considerably from the experimental ones and are not quoted here. Nevertheless, a nearly perfect error compensation brings the calculated changes of the rotational constants close to the experimental values. Anyhow, no geometric parameters are extracted from these calculations, which should merely be used to obtain good starting values for the GA fit. The CASSCF (10,10) calculations yield a mean ring CC bond length of 143.0 pm in the electronically excited state, compared to 143.8 pm from the fit of the geometry to the rotational constants. The pronounced quinoidal structure with C_2C_3 shorter than C_1C_2 and C_3C_4, which is predicted from the experimental rotational constants is not reproduced in the CASSCF calculations. Instead, these calculations yield a quite uniform increase of the aromatic ring bond lengths. The C_1O_7 bond length decreases upon electronic excitation both in the calculations and in the experiment, although the experimentally determined decrease is substantially larger. The same is found for the C_4Cl_8 bond, which decreases by

Table 4

Substitution coordinates (in pm) in 4-chlorophenol, 4-fluorophenol, and phenol in both electronic states

Compound	Atom	S_0		S_1	
		a	*b*	*a*	*b*
4-Chlorophenol	Cl	263.7(2)	0.3(2)	259.9(6)	0.9(6)
4-Chlorophenol	H	359.2(3)	83.1(2)	355.8(7)	85.5(6)
4-Fluorophenol	H	312.8(1)	79.4(1)	308.5(1)	79.6(1)
Phenol	H	258.6(1)	85.3(2)	259.1(2)	86.4(3)

Table 5
Comparison of experimental rotational constants and geometry parameters of 4-chlorophenol with the results of ab initio calculations

	S_0			S_1		
	Exp.	MP2	CASSCF	Exp.	CIS-HF	CASSCF
A''	5632.8	5637.6	5626.2	–	–	–
B''	975.6	971.0	968.1	–	–	–
C''	831.6	828.3	826.0	–	–	–
A'	–	–	–	5289.0	–	5295.2
B'	–	–	–	990.3	–	960.5
C'	–	–	–	834.4	–	813.0
ΔA	–	–	–	−343.8	−317.5	−331.2
ΔB	–	–	–	14.7	13.9	−7.6
ΔC	–	–	–	2.7	3.2	−13.0
C_1C_2	140.0(9)	139.7	139.1	146.5(9)	–	143.3
C_2C_3	139.8(1)	139.5	139.5	141.7(20)	–	143.0
C_3C_4	139.5(9)	139.3	138.9	143.3(9)	–	143.1
C_4Cl_8	172.8(3)	174.1	174.6	165.3(26)	–	173.0
C_1O_7	136.5(2)	137.2	135.4	130.0(30)	–	134.8
O_7H_{7a}	96.0	97.0	94.2	98.0	–	94.3
$C_{ar}H$	108.1	108.4	107.4	107.2	–	107.2
$C_2C_1O_7$	124(2)	123.1	122.4	122	–	121.7
$C_1O_7H_{7a}$	106(2)	108.6	111.1	110	–	111.2

All calculations have been performed with the 6-31G(d,p) basis set. The active space (10,10) used for the CASSCF calculations is described in Section 3.

7 pm according to the r_0 fit (6 pm according to the Kraitchman analysis), while the CASSCF calculations yield a shortening of only 1.6 pm.

6. Conclusions

We assigned the rotationally resolved electronic spectra of four different isotopomers of *p*-chlorophenol using an automated fitting strategy based on genetic algorithms. A quinoidal distortion of the aromatic ring upon electronic excitation was found, accompanied by a shortening of the (para) C—O and C—Cl bonds. Especially the experimentally determined decrease of the C—Cl bond length (−6 pm) is considerably larger than predicted from the CASSCF calculations (−1.6 pm). The same trend is found in the Franck–Condon analysis of Ref. [12], with a decrease of 2.4 pm. Since both Kraitchman analysis and fit of the structure to the rotational constants yield the same (large) reduction of the C—Cl bond length the larger value found in our analysis seems reliable.

The barrier to the internal rotation of the hydroxy group in the electronically excited state is determined to be 1400 cm^{-1}. This is only about 250 cm^{-1} higher than the corresponding value in the ground state. If one compares the ordering of torsional barriers in various para-substituted phenols, there is a substantial difference between the ground state and the excited state ordering. For the ground state the torsional barriers increase in the order F < CH$_3$ < Cl < H < CN, while for the excited state the ordering is Cl < F < CH$_3$ < H < CN. While in the electronic ground state, the torsional barrier of p-chlorophenol is higher than that of *p*-fluorophenol and *p*-methylphenol, the barrier of *p*-chlorophenol in the excited state is the lowest one. The reason for the ordering of the barriers of the halogenophenols in the ground state is the increase of the electron-withdrawing −I-effect, which is larger for fluorine compared to chlorine. This electron-withdrawing (inductive) effect stabilizes quasi-quinoidal structures with partial double bond character in the CO bond, thus increasing the torsional barrier. Additionally, the inductive effects are counterbalanced by a +M-effect, which increases in the same direction and leads to a decrease of the torsional barrier, since it destabilizes the quasi-quinoidal structures. This sensitive equilibrium of inductive and mesomeric effects of the substituents changes upon electronic excitation. While in the electronic ground state the overlap of the fluorine 2p$_z$ with the respective aromatic 2p$_z$ orbital is larger than for the 3p$_z$ of chlorine, in the excited state the π* orbitals can overlap more favorably with the p$_z$ orbitals of the chlorine substituent. Therefore the +M-effect of chlorine in *p*-fluorophenol increases in the excited state, thus decreasing the torsional barrier.

References

[1] W. Zierkiewicz, D. Michalska, P. Hobza, Chem. Phys. Lett. 386 (2004) 95–100.
[2] C. Ratzer, M. Nispel, M. Schmitt, Phys. Chem. Chem. Phys. 5 (2002) 812–819.
[3] J. Küpper, M. Schmitt, K. Kleinermanns, Phys. Chem. Chem. Phys. 4 (2002) 4634–4639.

[4] N.W. Larsen, J. Mol. Struct. 144 (1986) 83.

[5] W. Fateley, G. Carlson, F. Bentley, J. Phys. Chem. 79 (1975) 199.

[6] T. Cvitaš, J. Hollas, Mol. Phys. 18 (1970) 101.

[7] T. Cvitaš, J. Hollas, Mol. Phys. 18 (1970) 261.

[8] T. Cvitaš, J. Hollas, Mol. Phys. 18 (1970) 793.

[9] T. Cvitaš, J. Hollas, Mol. Phys. 18 (1970) 801.

[10] T. Cvitaš, J. Hollas, G. Kirby, Mol. Phys. 19 (1970) 305.

[11] J. Christoffersen, J.M. Hollas, G.H. Kirby, Mol. Phys. 18 (1970) 451.

[12] P. Imhof, D. Krügler, R. Brause, K. Kleinermanns, J. Chem. Phys. 121 (1999) 2598–2610.

[13] M. Schmitt, J. Küpper, D. Spangenberg, A. Westphal, Chem. Phys. 254 (2000) 349–361.

[14] S. Gerstenkorn, P. Luc, Atlas du spectre d'absorption de la molécule d'iode 14,800–20,000 cm^{-1}, CNRS, Paris, 1986.

[15] M.J. Frisch, G.W. Trucks, H.B. Schlegel, G.E. Scuseria, M.A. Robb, J.R. Cheeseman, V.G. Zakrzewski, J.A. Montgomery, Jr., R.E. Stratmann, J.C. Burant, S. Dapprich, J.M. Millam, A.D. Daniels, K.N. Kudin, M.C. Strain, O. Farkas, J. Tomasi, V. Barone, M. Cossi, R. Cammi, B. Mennucci, C. Pomelli, C. Adamo, S. Clifford, J. Ochterski, G.A. Petersson, P.Y. Ayala, Q. Cui, K. Morokuma, P. Salvador, J.J. Dannenberg, D.K. Malick, A.D. Rabuck, K. Raghavachari, J.B. Foresman, J. Cioslowski, J.V. Ortiz, A.G. Baboul, B.B. Stefanov, G. Liu, A. Liashenko, P. Piskorz, I. Komaromi, R. Gomperts, R.L. Martin, D.J. Fox, T. Keith, M.A. Al-Laham, C.Y. Peng, A. Nanayakkara, M. Challacombe, P.M.W. Gill, B. Johnson, W. Chen, M.W. Wong, J. Andres, C. Gonzalez, M. Head-Gordon, E.S. Replogle, J.A. Pople, Gaussian 98, revision a.11, Gaussian, Inc., Pittsburgh, PA (2001).

[16] W.L. Meerts, M. Schmitt, G. Groenenboom, Can. J. Chem. 82 (2004) 804–819.

[17] J.A. Hageman, R. Wehrens, R. de Gelder, W.L. Meerts, L.M.C. Buydens, J. Chem. Phys. 113 (2000) 7955–7962.

[18] D. Levine, PGAPack V1.0, PgaPack can be obtained via anonymous ftp from: ftp://ftp.mcs.anl.gov/pub/pgapack/pgapack.tar.z (1996).

[19] H.C. Allen, P.C. Cross, Molecular Vib-Rotors, Wiley, New York, 1963.

[20] J.H. Holland, Adaption in Natural and Artificial Systems, The University of Michigan Press, Ann-Arbor, MI, 1975.

[21] D.E. Goldberg, Genetic Algorithms in Search, Optimisation and Machine Learning, Addison-Wesley, Reading MA, 1989.

[22] I. Rechenberg, Evolutionsstrategie—Optimierung technischer Systeme nach Prinzipien der biologischen Evolution, Frommann-Holzboog, Stuttgart, 1973.

[23] C. Ratzer, J. Küpper, D. Spangenberg, M. Schmitt, Chem. Phys. 283 (2002) 153–169.

[24] M. Schmitt, D. Krügler, M. Böhm, C. Ratzer, V. Bednarska, I. Kalkman, W.L. Meerts, PCCP 8 (2006) 228–235.

[25] J. Kraitchman, Am. J. Phys. 21 (1953) 17.

[26] C. Costain, J. Chem. Phys. 29 (1958) 864.

[27] N.W. Larsen, F.M. Nicolaisen, J. Mol. Struct. 22 (1974) 29.

[28] G. Myszkiewicz, W.L. Meerts, C. Ratzer, M. Schmitt, J. Chem. Phys. 123 (2005) 044304–1–044304–7.

[29] G. Berden, W.L. Meerts, M. Schmitt, K. Kleinermanns, J. Chem. Phys. 104 (1996) 972–982.